JOURNAL OF AIRCRAFT
Vol. 46, No. 1, January–February 2009

Engineering Notes

ENGINEERING NOTES are short manuscripts describing new developments or important results of a preliminary nature. These Notes should not exceed 2500 words (where a figure or table counts as 200 words). Following informal review by the Editors, they may be published within a few months of the date of receipt. Style requirements are the same as for regular contributions (see inside back cover).

Numerical Optimization of Airfoils in Low Reynolds Number Flows

D. Nelson*
Los Angeles Air Force Base, El Segundo, California 90245

DOI: 10.2514/1.36859

Nomenclature

C_d = coefficient of drag
C_l = coefficient of lift
C_p = coefficient of pressure
c = chord
L/D = lift-to-drag ratio
Re = Reynolds number
α = angle of attack

Introduction

THE aerodynamic efficiency of an aircraft, or the ratio of the coefficient of lift to the coefficient of drag, is the most important parameter affecting the range and endurance of subsonic aircraft. For aircraft designed for the maximum range or endurance possible, it is therefore critical to achieve the highest possible lift-to-drag ratio. Unmanned aerial vehicles (UAV) are often designed for these types of long endurance/maximum range missions, including military surveillance UAVs requiring long loiter times or unpowered sailplanes looking for a long range or glide distance. Although there has been much research done on designing airfoils with very low coefficients of drag at transonic speeds [1–3] and at Reynolds numbers commonly encountered by lighter general aviation aircraft [4], there have been few research projects aimed at producing highly efficient airfoils for much smaller aircraft. Therefore, this Note uses numerical optimization in an attempt to design highly efficient airfoils for use on aircraft with spans of 2 to 3 m and operating around 10–40 mph, roughly at Reynolds numbers between 1×10^5 and 4×10^5. The resulting airfoils were then examined to determine their potential usefulness as wings and to explore what shapes and characteristics are most efficient at these low Reynolds numbers.

Other investigations into numerical optimization of airfoils for this Reynolds number range have been conducted by Secanell et al. [5], although their efforts concentrated on Reynolds numbers from 5×10^5 to 1.4×10^6. Secanell et al. also limited the maximum thickness-to-chord ratio to be 1%. Another investigation by Secanell and Suleman [6] used three different gradient-based optimization techniques to determine which would produce an airfoil with the lowest drag from a common starting airfoil. The Reynolds number in this case was 5×10^5, closer to this Note's target Reynolds numbers, although the thickness ratio was again constrained to 1%. This very low maximum thickness vale meant all the optimized airfoils that Secanell et al. [5,6] produced had a thickness-to-chord ratio of 1%, making them impractical airfoils for use in a real wing.

A more recent effort by Secanell et al. [7] focused on the design of airfoils for a small reconnaissance UAV; several airfoils were designed using optimization methods for all of the flight regions the UAV was expected to encounter, including takeoff, climb, cruise, loiter, and stall. This extended the Reynolds number region from 5×10^4 to 1.5×10^6. The gradient-based optimization routine used by Secanell et al. performed very similarly to the optimization routine used in this paper; both were given a fixed C_l and Reynolds number value and told to minimize drag. In response, the optimization routine minimized the airfoil's thickness and increased the camber. Secanell et al. concluded the optimization program was cutting thickness to reduce pressure drag. Unlike their earlier papers, Secanell et al. limited thickness to 5%. Interestingly, although this paper used a higher minimum thickness value, the resulting airfoils have higher aerodynamic efficiency values.

Another paper dealing with optimization of airfoils in low Reynolds numbers with direct implications on this paper is Lutz et al. [8], which optimized airfoils at Reynolds numbers of 2, 3, and 4×10^5. A hybrid genetic algorithm/gradient-based method using inverse airfoil design was used to minimize the drag coefficient at various coefficients of lift from 0.0 to 0.6. These values are very close to the target C_l and Reynolds number used in this investigation; however, different optimization and airfoil design methods are used in this Note, one of the suggestions for further research made by Lutz et al.

Methods

State-of-the-Art High Efficiency Low Reynolds Number Airfoils

The recent development and use of small unmanned aerial vehicles marks the first serious commercial and military use of aircraft that operate in the low Reynolds number regions of 50,000 to 200,000. Consequently, research and development of these aircraft has lagged behind other areas of aerodynamic research. However, much progress in this field has been made by amateur radio-controlled glider enthusiasts. Therefore, to determine the optimized airfoils' usefulness, several airfoils used on high-performance radio-controlled sailplanes were used as the control airfoils. Seven gliders were looked at, five with 2 m wingspans, and two more with 2.5 and 3 m spans.†

The most common airfoils used were the SA 7035 and the SD 7037, each being used on two gliders. However, the most efficient airfoil was the HQ 309, with a maximum lift-to-drag ratio of over 80 at a Reynolds number of 2×10^5 (Fig. 1). The other airfoil, the HQ 158, had the lowest lift-to-drag ratio of all the airfoils and the worst performance over all angles of attack. Therefore, the SD 7037 and the HQ 309 were used as control airfoils. The SA 7035 was not used as it has very similar performance albeit slightly worse than the SD 7037. All of these airfoils except the HQ 158 have a 9% thickness-to-chord ratio; to ensure a comparable test, the optimization program was constrained to a minimum thickness

Received 28 January 2008; revision received 22 July 2008; accepted for publication 22 July 2008.

*Captain, USAF, 501 Esplanade #304, Redondo Beach, CA 90277; daniel.nelson@losangeles.af.mil.

†Northeast Sailplane Products, http://www.nesail.com/categories.php?subcatID=3 [retrieved June 2006].

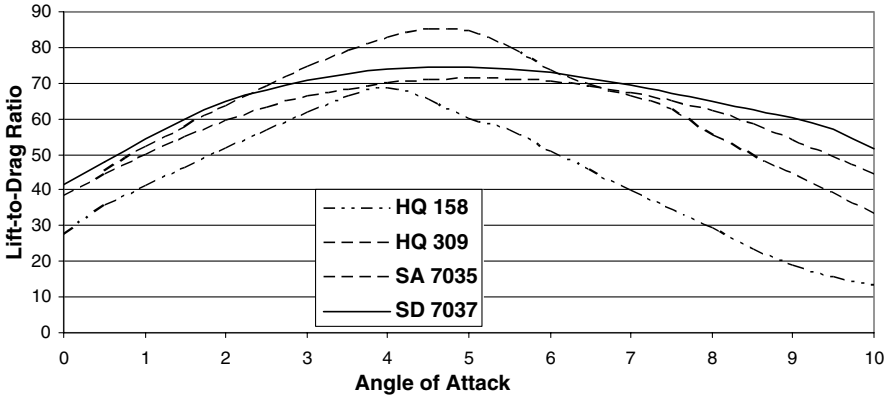

Fig. 1 Lift-to-drag ratio vs angle of attack for various state-of-the-art airfoils. $Re = 2 \times 10^5$.

ratio of 9%. This constraint did not preclude the possibility of thicker airfoils, however.

Airfoil Design Program

The numerical optimization scheme used here is commonly known as a direct-gradient method. This method attempts to design an airfoil by modifying several design parameters that directly affect the shape of the airfoil. A computational fluid dynamics program or some other airfoil analyzation tool is used to find the drag of the airfoil, and then a numerical optimization scheme is employed to modify the design parameters with the goal of reducing drag. For this project, the airfoil geometry is defined by a fifth-order polynomial Eq. (1):

$$y = a\sqrt{x} + bx + cx^2 + dx^3 + ex^4 + fx^5 \tag{1}$$

The coefficients a, b, c, d, e, and f control the shape of the equation's curve and are the design variables for the program. Using this equation once for the bottom surface and once for the top surface gives a total of 12 design variables. However, for y to be 0 at x values of 0 and 1 (corresponding to the leading and trailing edge), b must be equal to negative a, d must be equal to negative c, and f must be equal to negative e. This cuts the amount of design parameters down to six.

A numerical optimization scheme known as steepest descent was used to optimize the design variables. This method finds the gradient of a function at a point and takes a step in the opposite direction Eq. (2). The method of steepest descent is unconditionally stable, although depending on the starting conditions it can take an infinite number of iterations to reach the function's minimum. Depending on the step size λ_k it can also oscillate around the optimization function's minimum. Fortunately, the minimum drag for an airfoil in viscous flow is zero pressure drag (corresponding to a one-dimensional flat plate) plus some amount of skin friction drag. As this project is concerned with designing real airfoils, some internal thickness and consequently some pressure drag must be present; thus the absolute minimum will not be reached:

$$x_{k+1} = x_k - \lambda_k \nabla f(x_k) \tag{2}$$

To constrain the airfoil design tool to a minimum thickness ratio, the maximum thickness was calculated each time a new airfoil was generated. If the new airfoil was thinner than the constraint (9% in this case), the program divided the step size λ_k by 10 and regenerated the airfoil. This process was repeated until the airfoil no longer violated the thickness constraint. Step size was not reset after each program iteration in order to reduce the possibility of the program oscillating around a local minimum. Although this probably increased the total number of iterations needed and overall run times, it did not do so prohibitively. The program was run until the total change in drag was less than one ten-thousandth. Occasionally, the program would settle in a local minimum, which was recognized when the resulting airfoil had a maximum thickness ratio of more then 9%. In this case, optimization could be continued by using the resulting airfoil's design variables as the starting variables for another program run; this usually resulted in further optimization of the airfoil.

Taken together, the airfoil shape equation and the gradient optimization scheme form the direct-gradient method. This method has been proven to give good results when used to design airfoils with minimal drag. However, it can produce airfoils with poor off-design performance. Although this is a concern, the aircraft that are intended to use the airfoils designed here spend the great majority of their mission operating at the maximum endurance or range airspeed; therefore, performance at off-design conditions is not as important as increasing maximum efficiency.

Drela and Youngren's X-Foil[‡] was chosen as the computational fluid dynamics routine. X-Foil has been used in other airfoil optimization efforts, notably Venkataraman's [9], and is very accurate, especially when used in low Reynolds number flows. However, as X-Foil is a two-dimensional code, the reported drag is only drag due to pressure and skin friction. When used to analyze an airfoil, X-Foil requires the user to input the desired Reynolds number and either the desired angle of attack or coefficient of lift. In this program, the lift coefficient at which optimization is carried out at is specified. Finally, a program was written using *C* linking X-Foil, the airfoil generation routine, and the optimization routine.

Examination of Optimized Airfoils

A few notes regarding the naming convention used here should be mentioned. The final optimized airfoils all have "ND" followed by five digits, where "D" refers to the parameter being minimized, in this case drag. The first two digits represent the design C_l value times 10, while the last three digits represent the design Reynolds number divided by 100. For example, ND 10360 represents an airfoil that was optimized to generate the minimum drag at a coefficient of lift of 1.0 at a Reynolds number of 3.6×10^5. If the coefficient of lift is below 1.0, the 0 in the one's place is included, so that ND 07200 represents an airfoil optimized at a C_l of 0.7 and a Reynolds number of 2×10^5.

Optimizing an Airfoil

Figure 2 shows the initial airfoil and the resulting airfoil the optimization program designed. As stated earlier, only pressure and friction drag can be estimated by X-Foil; therefore, the easiest way for the optimizer to reduce drag is to make the airfoil thinner, cutting both the frontal profile to reduce pressure drag and the overall wetted surface to reduce friction drag. This can be seen in Fig. 2, as thickness was reduced from 13.7% for the initial airfoil to the minimal thickness of 9% for the final, cutting the drag coefficient from 0.0113 to 0.01055. Interestingly, the optimization program also increased the amount of camber in the final airfoil, allowing it to reach a higher coefficient of lift values at lower angle of attacks than the flatter initial

[‡]Drela, M., and Youngren, H., "X-Foil 6.9 User Primer," XFoil Subsonic Airfoil Design System, http://web.mit.edu/drela/Public/web/xfoil/ [retrieved June 2006].

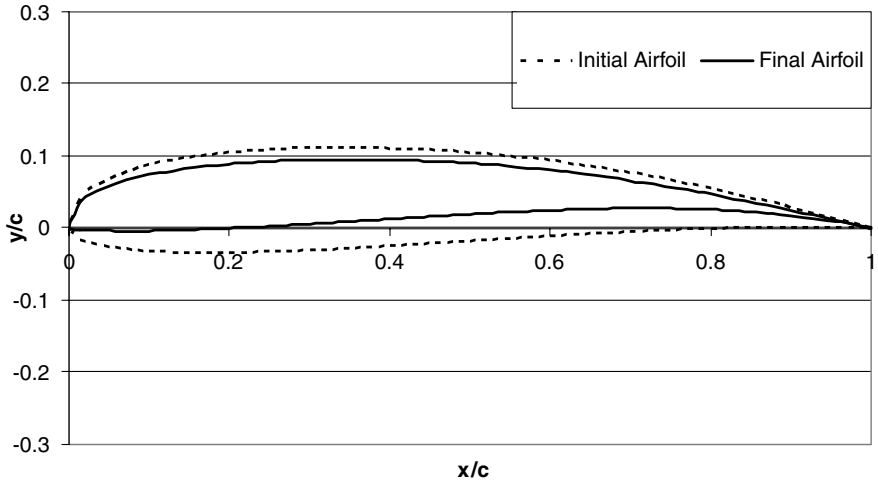

Fig. 2 Optimization of an airfoil.

airfoil and further reducing pressure drag. This resulted in an increase of the maximum lift-to-drag ratio from 72 to 96. The optimization program was run at a coefficient of lift of 1.0 and a Reynolds number of 2×10^5, so this airfoil is a ND 10200. Eighteen iterations were needed for the airfoil optimization program to reach the final airfoil.

Effects of Changing Design Coefficient of Lift

As X-Foil requires the user to define the coefficient of lift and Reynolds number, several tests were performed by changing the design coefficient of lift to determine which values caused the optimization program to output the most efficient airfoils. The same initial airfoil shown in Fig. 2 was used again with the lift coefficient set to 0.5, 0.8, and 1.0. The Reynolds number was again set to 2×10^5.

The results show that the most efficient airfoils are produced when the design lift coefficient is high, around 1.0 (Table 1). The airfoil optimized at 1.0 has the most camber and the lowest thickness ratio (Fig. 3), as well as the highest lift-to-drag ratio. Interestingly, it also has the highest minimum drag. This suggests that when designing highly efficient airfoils, the main focus should be to reduce the amount of drag generated per amount of lift the airfoil generates, not reducing drag at all costs.

It should be noted that, even with the same initial conditions and starting points, an optimization program can arrive at different final solutions. This is especially true of the steepest descent method, which has a tendency to settle into a local minimum. The two different ND 10200s examined so far show this behavior. The airfoil optimized during the initial test is 9% thick with a lift-to-drag ratio of 96, while the ND 10200 optimized during the C_l test is 10% thick with a lift-to-drag ratio of 88. The user is thus cautioned to perform several runs with an optimization program using the same initial conditions to be sure the program is arriving at the best possible answer.

Effects of Changing Design Reynolds Number

To further explore the question of what airfoil shapes are the most efficient at this Reynolds number range, several runs of the optimization program were performed at different Reynolds number while keeping the design coefficient of lift constant. As previous tests showed that optimizing at higher C_l produced the best results, the coefficient of lift was set to 1.0. The Reynolds numbers used were 1, 2, 3.6, and 4.5×10^5. The initial airfoil shown in Fig. 2 was used as the starting point for this test also. The resulting airfoils (Fig. 4) show that the optimization program added more camber to the airfoils as the Reynolds number was increased from 1×10^5 to 4.5×10^5. However, besides the different camber, all the final airfoils have generally the same shape: a thick, rounded leading edge and a thin, highly cambered trailing edge. These characteristics can also be seen in the optimized airfoils shown in Figs. 2 and 3.

Table 1 C_d and L/D for airfoils optimized at various C_l

Design C_l	Minimum C_d	Maximum L/D	Thickness
C_l 0.5	0.0097	62	12.60%
C_l 0.8	0.0101	80	11.40%
C_l 1.0	0.0117	88	10.60%

As the optimization process was performed at several different Reynolds numbers, the resulting optimized airfoils were also analyzed as different Reynolds numbers (1, 2, and 4×10^5). However, no clear conclusion could be drawn from the resulting drag coefficient and lift-to-drag ratio data. The ND 10100, while optimized at $Re = 1 \times 10^5$, had the worst performance at all Reynolds numbers, whereas the ND 10450 had the second worst performance at 1×10^5 but the best performance at $Re = 4 \times 10^5$. Two airfoils optimized at 2×10^5 and 3.6×10^5 had very good performance overall, although the ND 10200 was more suited to lower Reynolds numbers while the ND 10360 was better at higher Reynolds numbers. Therefore, the only recommendation that can be made is to run the optimization program at several different Reynolds numbers at and around the aircraft's expected cruise Reynolds number and then analyze the resulting airfoils to determine which is best suited for the aircraft.

Comparison of Existing Airfoils to Optimized Airfoils

A comparison of the selected state-of-the-art existing airfoils (represented by the SD 7037) and the optimized airfoils (represented by the ND 11200) (Fig. 5) shows the ND airfoils have a rounder leading edge and more camber, especially in the trailing edge. The lower surface of the ND 11200 also shows a much greater concave shape than the existing airfoils, with an inflection point around 10% of the chord and crossing the x axis at 20%. The lower surface on the SD 7037 also shows an inflection point and a concave shape; however, this happens much later than the optimized airfoils, with the inflection point occurring around 20% of the chord and crossing the x axis around 80%.

The existing and optimized airfoils were then analyzed at Reynolds numbers of 1, 2, and 4×10^5. Each airfoil's minimum drag coefficient and maximum lift-to-drag ratio (Table 2) were found and compared. The existing airfoils all have much less drag across the entire Reynolds number region than the optimized airfoils due to a lower chord line and less camber. However, the optimized airfoils all have greater maximum lift-to-drag ratios.

Additionally, the optimized airfoils show a higher lift-to-drag ratio at lower angles of attack than the existing airfoils. This difference is readily apparent in Figs. 6 and 7. This tendency of the optimized airfoils to reach their maximum lift-to-drag ratio at lower angles of

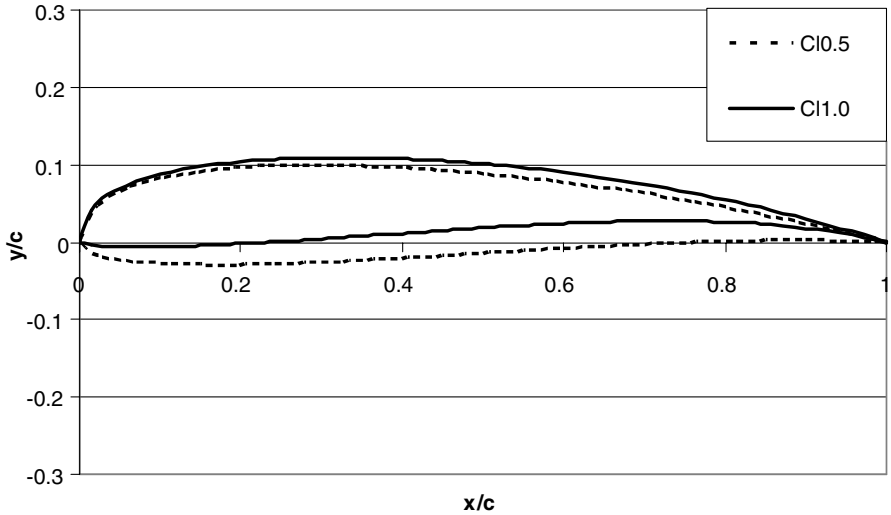

Fig. 3 Optimization at different C_l.

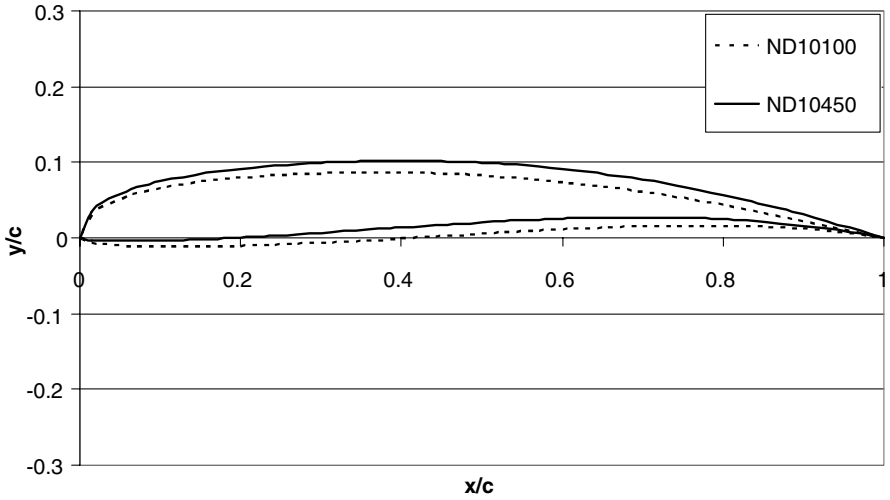

Fig. 4 Final optimized airfoils after varying design Reynolds number.

attack than the existing airfoils is also valuable, as cruising at a lower angle of attack requires less pitch trim and therefore generates less trim drag. At higher angles of attack, the existing and optimized airfoils all have about the same efficiency.

One surprising observation is that while Table 2 shows the SD 7037 has the least drag across the full range of Reynolds numbers, the aerodynamic efficiency charts shows that it also has the lowest maximum lift-to-drag ratio. Plotting the drag polars of the selected airfoils (Fig. 8) shows that while the SD 7037 has the lowest drag coefficients, it is achieving these values at relatively low coefficients of lift. The optimized airfoils do have more drag but achieve these drag coefficients at much higher coefficients of lift. This confirms the

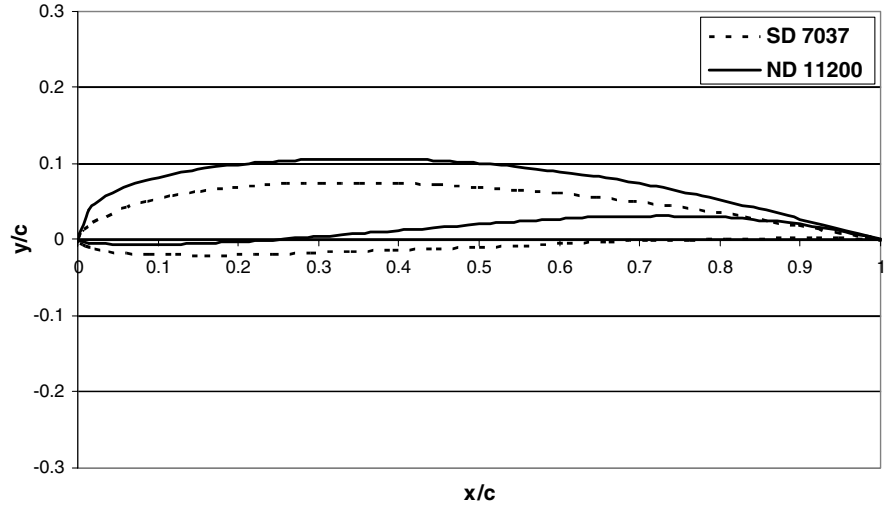

Fig. 5 SD 7037 and ND 11200.

Table 2 Minimum coefficient of drag and maximum lift-to-drag ratio at various Reynolds numbers

	$Re = 1 \times 10^5$		$Re = 2 \times 10^5$		$Re = 4 \times 10^5$	
Airfoil	Min C_d	Max L/D	Min C_d	Max L/D	Min C_d	Max L/D
SD 7037	0.0146	55	0.009	74	0.0061	93
HQ 309	0.0156	61	0.0098	85	0.0065	108
ND 11200	0.0174	68	0.0111	97	0.0086	123
ND 10360	0.0181	69	0.0109	99	0.0075	131

notion that, when designing airfoils with very high lift-to-drag ratios, the objective should not be to simply minimize the drag coefficient, but to increase the amount of lift the airfoil can generate per additional amount of drag. As expected with the direct-gradient optimization method, the optimized airfoils have relatively poor performance away from the design coefficient of lift as shown by the narrow "drag bucket." Still, even with the tendency for poor off-design point performance, the ND 11200 airfoil has better efficiencies than the existing airfoils and would be the better choice for use on a real wing. That this only becomes clear after examining the aerodynamic efficiency vs angle of attack plot (Figs. 6 and 7) indicates this graph can be a valuable tool when designing long endurance aircraft.

Analysis of Pressure Coefficient Distributions Along Existing and Optimized Airfoils

A major problem in low Reynolds number flows is the presence of local areas of separation along the airfoil, called separation bubbles. These bubbles increase the boundary layer thickness and increase pressure drag across the airfoil; one design goal of low Reynolds number airfoils is therefore to minimize or eliminate their occurrence.

Separation bubbles are formed when the boundary layer is subjected to adverse pressure gradients during the pressure recovery stage along the upper surface of the airfoil. Although all airfoils experience a pressure recovery area, separation bubbles are usually more of a problem in low Reynolds number flows as the boundary layer along the airfoil tends to stay laminar much longer than at higher Reynolds numbers. This laminar boundary layer is much more susceptible to separation due to adverse pressure gradients than a turbulent boundary layer. Although some skin friction drag savings is realized by having laminar flow instead of turbulent, the increase in pressure drag due to the separation bubble more then offsets any reduction in friction drag.

Plotting the distribution of the pressure coefficient along the HQ 309 and ND 11200 at maximum aerodynamic efficiency (Figs. 9 and 10), the most immediate difference is the modern airfoil has a very sharp increase to the maximum negative pressure coefficient followed by a sharp decrease, whereas the optimized airfoil has a smoother curve and a more gradual decrease in the pressure coefficient. Both airfoils have a small bump representing the separation bubble; however, the faster pressure recovery shown by the HQ 309 causes a greater adverse pressure gradient than the more gradual recovery seen by the ND 11200, and consequently, the

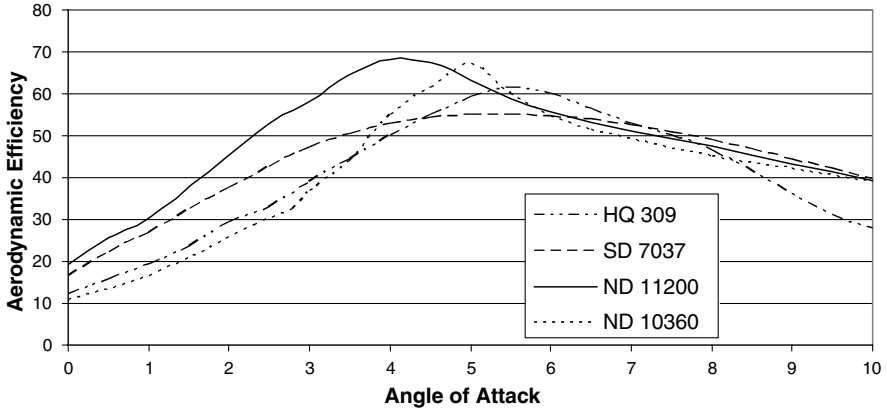

Fig. 6 Aerodynamic efficiency vs angle of attack, $Re = 1 \times 10^5$.

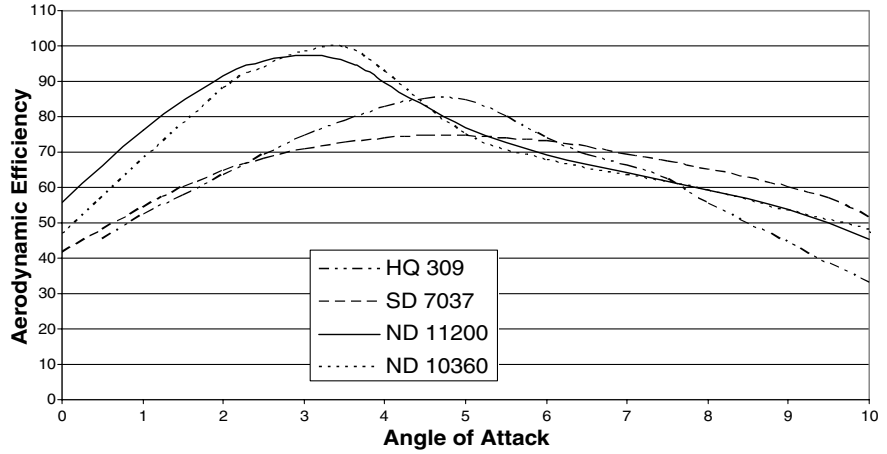

Fig. 7 Aerodynamic efficiency vs angle of attack, $Re = 2 \times 10^5$.

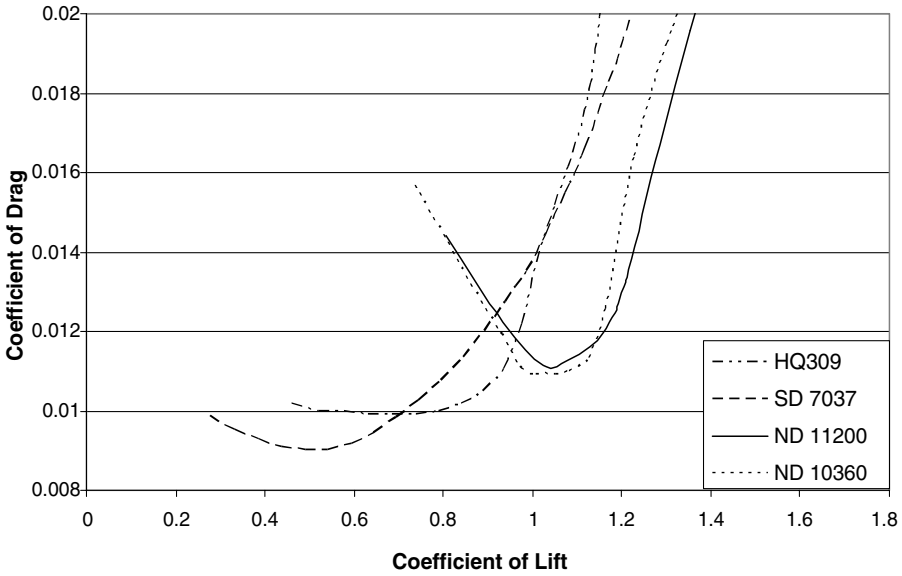

Fig. 8 Drag polar of selected airfoils. $Re = 2 \times 10^5$.

separation bubble is smaller. This is due to the ND 11200's blunt leading edge. As the angle of attack is increased and the front stagnation point moves onto the lower surface, the airflow must accelerate faster to get around a sharper leading edge, placing the point of maximum suction very close to the leading edge as seen in Fig. 9. Once the flow passes this point, it must decelerate quickly in order to follow the airfoil's surface. Conversely, in Fig. 10 the maximum suction point is slightly aft of the ND 11200's leading edge, giving the flow more time to accelerate. Once past the maximum suction point, the rounded leading edge lets the flow decelerate slower, setting up a lower adverse pressure gradient than in the HQ 309.

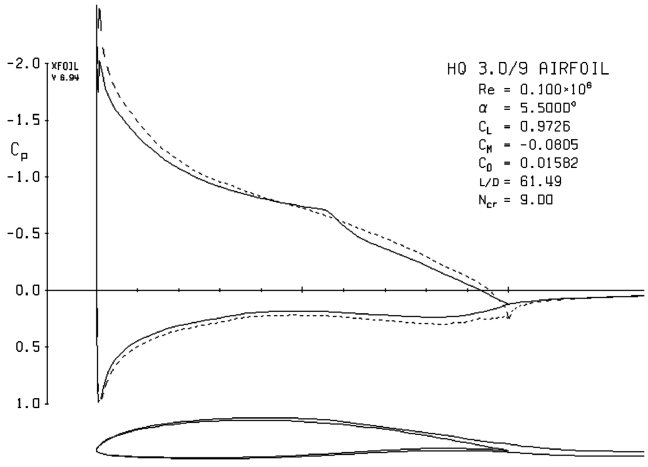

Fig. 9 C_p distribution, HQ 309.

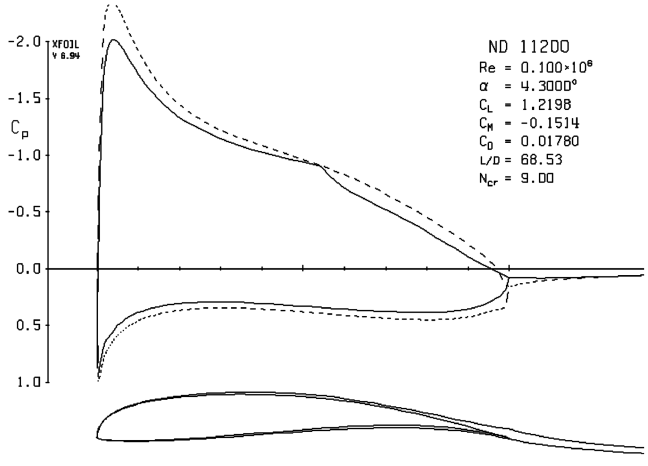

Fig. 10 C_p distribution, ND 11200.

Conclusions

The recent interest in small unmanned aerial vehicles by the military for surveillance and other missions requiring long endurance times has resulted in many companies filling this role by adapting commercially available radio-controlled aircraft technologies to the military's requirements. However, as the small military UAV is rather new, most radio-controlled aircrafts are designed around older airfoils. This investigation therefore applied numerical optimization design methods to design newer, more efficient airfoils for use in the next generation small UAVs.

The direct-gradient optimization method was coupled to an airfoil generator using a fifth-order polynomial. X-Foil was used to analyze the resulting airfoils. The airfoils generated were compared to modern airfoils used in high-performance radio-controlled sailplanes. The optimizer-designed airfoils were found to have higher lift-to-drag ratios than the modern airfoils, in some cases almost 20% higher. These gains in efficiency will directly result in longer endurance times. Although the method presented here is simple, easy to implement, and generates good results, there are areas that could benefit from refinement. Specifically, the airfoil generation tool is very simple; there may be airfoil geometries that the fifth-order polynomial used here is not able to represent. Therefore, some characteristics common to the airfoils generated here, such as the blunt leading edge, may be a result of the polynomial's limitations and not the end result of the optimization process. An interesting approach would be to use the y coordinate of the airfoil's surface as the design variables. Although this would greatly increase the number of design variables, it would give the airfoil design tool complete freedom to generate any possible airfoil shape.

Another result is the use of the aerodynamic efficiency vs angle of attack chart for airfoil selection. The optimized airfoils designed here had higher drag coefficients than the modern airfoils and the drag polar plots showed a narrow drag bucket. From just the drag polar chart, the choice of airfoils for a real wing is not clear; however, the aerodynamic efficiency vs angle of attack chart directly shows which airfoils give better performance over a range of angle of attack values, as well as the angle of attack for maximum efficiency.

Because endurance depends on the ratio of lift cubed to drag squared, the graph could be converted to show the correct angle of attack for maximum endurance as well.

References

[1] Haney, H., and Johnson, R., "Computational Optimization and Wind Tunnel Test of Transonic Wing Designs," *Journal of Aircraft*, Vol. 17, No. 7, 1980, pp. 457–463. doi:10.2514/3.57925

[2] Li, W., Krist, S., and Campbell, R., "Transonic Airfoil Shape Optimization in Preliminary Design Environment," AIAA Paper 2004-4629, 2004.

[3] Ray, T., and Tsai, H., "A Parallel Hybrid Optimization Algorithm for Robust Airfoil Design," AIAA Paper 2004-905, 2004.

[4] Barrett, T., Bessloff, N., and Keane, A., "Airfoil Design and Optimization Using Multi-Fidelity Analysis and Embedded Inverse Design," AIAA Paper 2006-1820, 2006.

[5] Secanell, M., Suleman, A., and Gamboa, P., "Design of a Morphing Airfoil for a Light Unmanned Aerial Vehicle Using High-Fidelity Aerodynamic Shape Optimization," AIAA Paper 2005-1891, 2005.

[6] Secanell, M., and Suleman, A., "Numerical Evaluation of Optimization Algorithms for Low-Reynolds-Number Aerodynamic Shape Optimization," *AIAA Journal*, Vol. 43, No. 10, 2005, pp. 2262–2267. doi:10.2514/1.12563

[7] Secanell, M., Suleman, A., and Gamboa, P., "Design of a Morphing Airfoil Using Aerodynamic Shape Optimization," *AIAA Journal*, Vol. 44, No. 7, July 2006, pp. 1550–1562. doi:10.2514/1.18109

[8] Lutz, T., Würz, W., and Wagner, S., "Numerical Optimization and Wind-Tunnel Testing of Low Reynolds-Number Airfoils," *Fixed and Flapping Wing Aerodynamics for Micro Air Vehicle Applications*, edited by T. J. Mueller, AIAA, Reston, VA, 2001, Vol. 195, pp. 169–191.

[9] Venkataraman, P., "Low Speed Multi-Point Airfoil Design," AIAA Paper 98-2402, 1998.